Generation of primordial non-Gaussianities and constraints from Planck

L. Sriramkumar

Department of Physics, Indian Institute of Technology Madras, Chennai

Field Theoretic Aspects of Gravity IX

Indian Institute of Technology, Gandhinagar

April 16, 2013

Proliferation of inflationary models[1]

5-dimensional assisted inflation
anisotropic brane inflation
anomaly-induced inflation
assisted inflation
assisted chaotic inflation
boundary inflation
brane inflation
brane-assisted inflation
brane gas inflation
brane-antibrane inflation
braneworld inflation
Brans-Dicke chaotic inflation
Brans-Dicke inflation
bulky brane inflation
chaotic hybrid inflation
chaotic inflation
chaotic new inflation
D-brane inflation
D-term inflation
dilaton-driven inflation
dilaton-driven brane inflation
double inflation
double D-term inflation
dual inflation
dynamical inflation
dynamical SUSY inflation
eternal inflation
extended inflation
extended open inflation
extended warm inflation
extra dimensional inflation
F-term inflation
F-term hybrid inflation
false vacuum inflation
false vacuum chaotic inflation
fast-roll inflation
first order inflation
gauged inflation
generalised inflation
generalized assisted inflation
generalized slow-roll inflation
gravity driven inflation
Hagedorn inflation
higher-curvature inflation
hybrid inflation
hyperextended inflation
induced gravity inflation
induced gravity open inflation
intermediate inflation
inverted hybrid inflation
isocurvature inflation
K inflation
kinetic inflation
lambda inflation
large field inflation
late D-term inflation
late-time mild inflation
low-scale inflation
low-scale supergravity inflation
M-theory inflation
mass inflation
massive chaotic inflation
moduli inflation
multi-scalar inflation
multiple inflation
multiple-field slow-roll inflation
multiple-stage inflation
natural inflation
natural Chaotic inflation
natural double inflation
natural supergravity inflation
new inflation
next-to-minimal supersymmetric hybrid inflation
non-commutative inflation
non-slow-roll inflation
nonminimal chaotic inflation
old inflation
open hybrid inflation
open inflation
oscillating inflation
polynomial chaotic inflation
polynomial hybrid inflation
power-law inflation
pre-Big-Bang inflation
primary inflation
primordial inflation
quasi-open inflation
quintessential inflation
R-invariant topological inflation
rapid asymmetric inflation
running inflation
scalar-tensor gravity inflation
scalar-tensor stochastic inflation
Seiberg-Witten inflation
single-bubble open inflation
spinodal inflation
stable starobinsky-type inflation
steady-state eternal inflation
steep inflation
stochastic inflation
string-forming open inflation
successful D-term inflation
supergravity inflation
supernatural inflation
superstring inflation
supersymmetric hybrid inflation
supersymmetric inflation
supersymmetric topological inflation
supersymmetric new inflation
synergistic warm inflation
TeV-scale hybrid inflation

A partial list of ever-increasing number of inflationary models!

[1] From E. P. S. Shellard, *The future of cosmology: Observational and computational prospects*, in *The Future of Theoretical Physics and Cosmology*, Eds. G. W. Gibbons, E. P. S. Shellard and S. J. Rankin (Cambridge University Press, Cambridge, England, 2003).

Plan of the talk

Inflation resolves the horizon problem

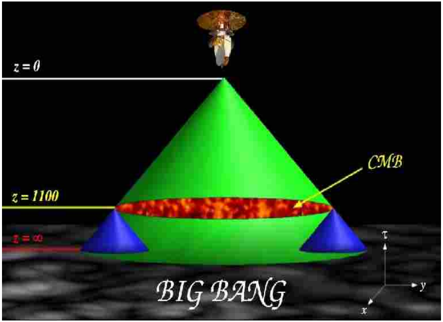

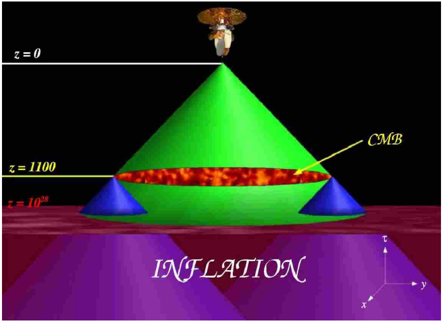

Left: The radiation from the CMB arriving at us from regions separated by more than the Hubble radius at the last scattering surface (which subtends an angle of about 1° today) could not have interacted before decoupling.

[2] Images from W. Kinney, astro-ph/0301448.

Inflation resolves the horizon problem

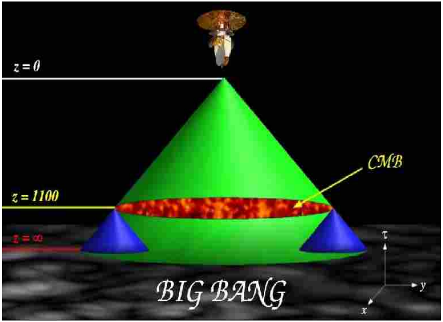

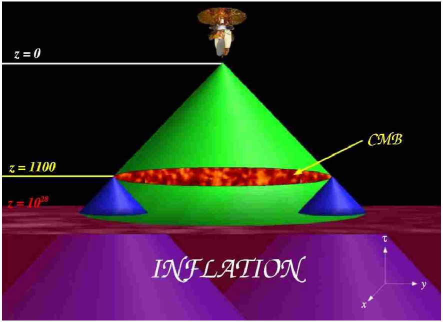

Left: The radiation from the CMB arriving at us from regions separated by more than the Hubble radius at the last scattering surface (which subtends an angle of about 1° today) could not have interacted before decoupling.
Right: An illustration of how an early and sufficiently long epoch of inflation helps in resolving the horizon problem[2].

[2] Images from W. Kinney, astro-ph/0301448.

Bringing the modes inside the Hubble radius

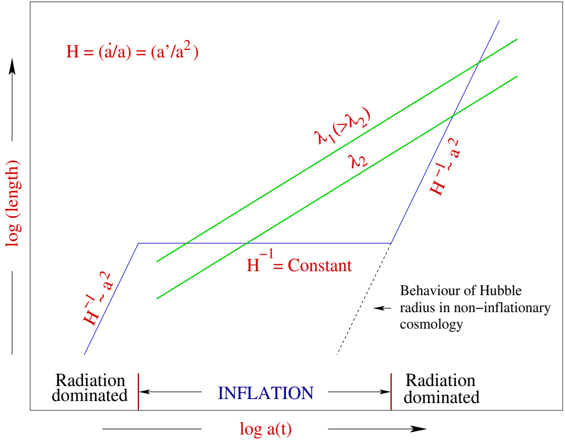

A schematic diagram illustrating the behavior of the physical wavelength $\lambda_{\rm P} \propto a$ (the green lines) and the Hubble radius H^{-1} (the blue line) during inflation and the radiation dominated epochs[3].

[3] See, for example, E. W. Kolb and M. S. Turner, *The Early Universe* (Addison-Wesley Publishing Company, New York, 1990), Fig. 8.4.

A variety of potentials to choose from

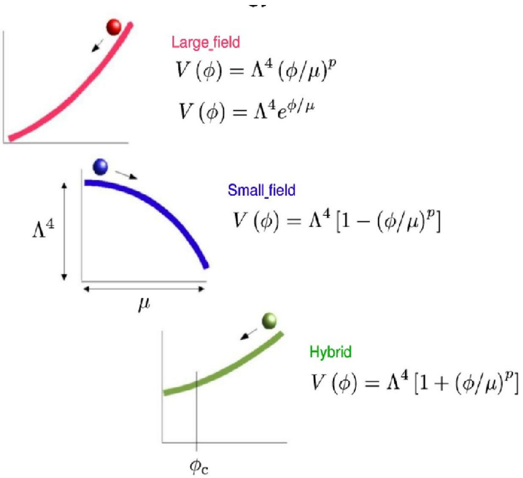

A variety of scalar field potentials have been considered to drive inflation[4]. Often, these potentials are classified as small field, large field and hybrid models.

[4] Image from W. Kinney, astro-ph/0301448.

The character of the perturbations

In a Friedmann universe, the perturbations in the metric and the matter can be classified according to their behavior with respect to a local rotation of the spatial coordinates on hypersurfaces of constant time as follows[5]:

- ✦ Scalar perturbations – Density and pressure perturbations
- ✦ Vector perturbations – Rotational velocity fields
- ✦ Tensor perturbations – Gravitational waves

[5] See, for instance, L. Sriramkumar, Curr. Sci. **97**, 868 (2009).

The character of the perturbations

In a Friedmann universe, the perturbations in the metric and the matter can be classified according to their behavior with respect to a local rotation of the spatial coordinates on hypersurfaces of constant time as follows[5]:

- Scalar perturbations – Density and pressure perturbations
- Vector perturbations – Rotational velocity fields
- Tensor perturbations – Gravitational waves

The metric perturbations are related to the matter perturbations through the first order Einstein's equations.

[5] See, for instance, L. Sriramkumar, Curr. Sci. **97**, 868 (2009).

The character of the perturbations

In a Friedmann universe, the perturbations in the metric and the matter can be classified according to their behavior with respect to a local rotation of the spatial coordinates on hypersurfaces of constant time as follows[5]:

- Scalar perturbations – Density and pressure perturbations
- Vector perturbations – Rotational velocity fields
- Tensor perturbations – Gravitational waves

The metric perturbations are related to the matter perturbations through the first order Einstein's equations.

Inflation does not produce any vector perturbations, while the tensor perturbations can be generated even in the absence of sources.

[5] See, for instance, L. Sriramkumar, Curr. Sci. **97**, 868 (2009).

The character of the perturbations

In a Friedmann universe, the perturbations in the metric and the matter can be classified according to their behavior with respect to a local rotation of the spatial coordinates on hypersurfaces of constant time as follows[5]:

- ✦ Scalar perturbations – Density and pressure perturbations
- ✦ Vector perturbations – Rotational velocity fields
- ✦ Tensor perturbations – Gravitational waves

The metric perturbations are related to the matter perturbations through the first order Einstein's equations.

Inflation does not produce any vector perturbations, while the tensor perturbations can be generated even in the absence of sources.

It is the fluctuations in the inflaton field ϕ that act as the seeds for the scalar perturbations that are primarily responsible for the anisotropies in the CMB and, eventually, the present day inhomogeneities.

[5] See, for instance, L. Sriramkumar, Curr. Sci. **97**, 868 (2009).

The scalar and the tensor perturbation spectra

The dimensionless scalar power spectrum $\mathcal{P}_{\mathrm{S}}(k)$ is defined in terms of the correlation function of the Fourier modes of the curvature perturbation $\hat{\mathcal{R}}_{\boldsymbol{k}}$ as follows:

$$\langle 0|\hat{\mathcal{R}}_{\boldsymbol{k}}(\eta)\,\hat{\mathcal{R}}_{\boldsymbol{k}'}(\eta)|0\rangle = \frac{(2\,\pi)^2}{2\,k^3}\,\mathcal{P}_{\mathrm{S}}(k)\,\delta^{(3)}\left(\boldsymbol{k}+\boldsymbol{k}'\right),$$

where $|0\rangle$ is often referred to as the Bunch-Davies vacuum.

The scalar and the tensor perturbation spectra

The dimensionless scalar power spectrum $\mathcal{P}_{_{\rm S}}(k)$ is defined in terms of the correlation function of the Fourier modes of the curvature perturbation $\hat{\mathcal{R}}_{\boldsymbol{k}}$ as follows:

$$\langle 0|\hat{\mathcal{R}}_{\boldsymbol{k}}(\eta)\,\hat{\mathcal{R}}_{\boldsymbol{k}'}(\eta)|0\rangle = \frac{(2\,\pi)^2}{2\,k^3}\,\mathcal{P}_{_{\rm S}}(k)\,\delta^{(3)}\,(\boldsymbol{k}+\boldsymbol{k}')\,,$$

where $|0\rangle$ is often referred to as the Bunch-Davies vacuum.

While comparing with the observations, for convenience, one often uses the following power law, template scalar and the tensor spectra:

$$\mathcal{P}_{_{\rm S}}(k) = \mathcal{A}_{_{\rm S}}\,\left(\frac{k}{k_\ast}\right)^{n_{_{\rm S}}-1} \quad \text{and} \quad \mathcal{P}_{_{\rm T}}(k) = \mathcal{A}_{_{\rm T}}\,\left(\frac{k}{k_\ast}\right)^{n_{_{\rm T}}},$$

with the spectral indices $n_{_{\rm S}}$ and $n_{_{\rm T}}$ assumed to be constant.

The scalar and the tensor perturbation spectra

The dimensionless scalar power spectrum $\mathcal{P}_{_{\rm S}}(k)$ is defined in terms of the correlation function of the Fourier modes of the curvature perturbation $\hat{\mathcal{R}}_{\boldsymbol{k}}$ as follows:

$$\langle 0|\hat{\mathcal{R}}_{\boldsymbol{k}}(\eta)\,\hat{\mathcal{R}}_{\boldsymbol{k}'}(\eta)|0\rangle = \frac{(2\,\pi)^2}{2\,k^3}\,\mathcal{P}_{_{\rm S}}(k)\,\delta^{(3)}\,(\boldsymbol{k}+\boldsymbol{k}')\,,$$

where $|0\rangle$ is often referred to as the Bunch-Davies vacuum.

While comparing with the observations, for convenience, one often uses the following power law, template scalar and the tensor spectra:

$$\mathcal{P}_{_{\rm S}}(k) = \mathcal{A}_{_{\rm S}}\,\left(\frac{k}{k_\ast}\right)^{n_{_{\rm S}}-1} \quad {\rm and} \quad \mathcal{P}_{_{\rm T}}(k) = \mathcal{A}_{_{\rm T}}\,\left(\frac{k}{k_\ast}\right)^{n_{_{\rm T}}}\,,$$

with the spectral indices $n_{_{\rm S}}$ and $n_{_{\rm T}}$ assumed to be constant.

The tensor-to-scalar ratio r is defined as

$$r(k) \equiv \frac{\mathcal{P}_{_{\rm T}}(k)}{\mathcal{P}_{_{\rm S}}(k)}$$

and it is usual to further set $r = -8\,n_{_{\rm T}}$, viz. the so-called consistency relation, which is valid during slow roll inflation.

Angular power spectrum from the WMAP 9-year data[6]

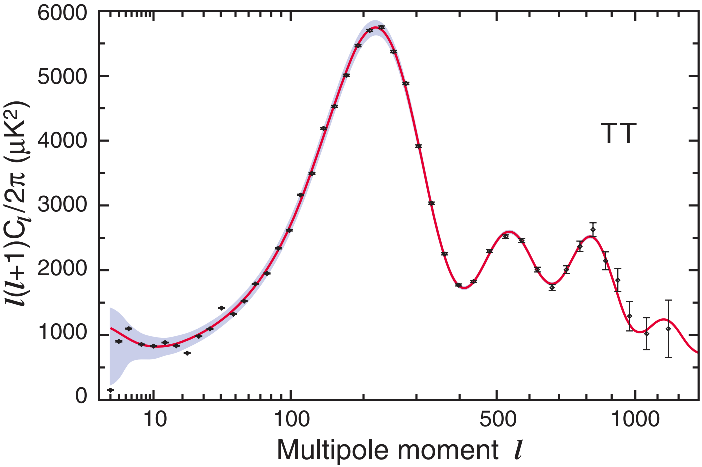

The WMAP 9-year data for the CMB TT angular power spectrum (the black dots with error bars) and the theoretical, best fit ΛCDM model with a power law primordial spectrum (the solid red curve).

[6] C. L. Bennett *et al.*, arXiv:1212.5225v1 [astro-ph.CO].

Angular power spectrum from the Planck data[7]

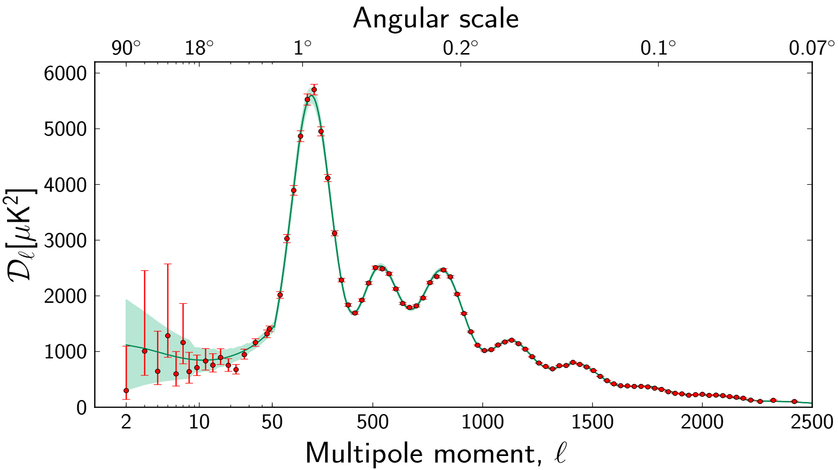

The CMB TT angular power spectrum from the Planck data (the red dots with error bars) and the theoretical, best fit ΛCDM model with a power law primordial spectrum (the solid green curve).

[7] P. A. R. Ade *et al.*, arXiv:1303.5075 [astro-ph.CO].

Constraints from the WMAP data[8]

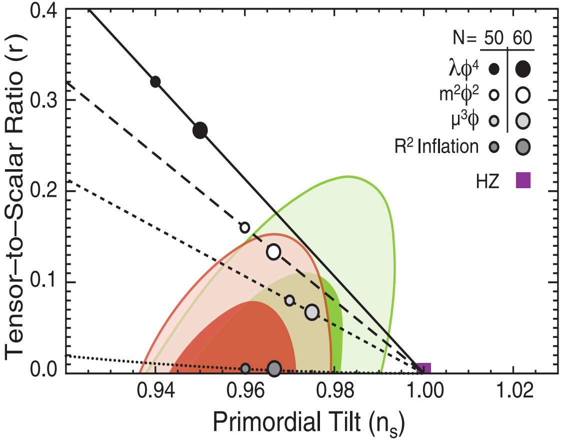

Joint constraints from the WMAP nine-year and other cosmological data on the inflationary parameters $n_{\rm s}$ and r for large field models with potentials of the form $V(\phi) \propto \phi^n$.

[8] G. Hinshaw *et al.*, arXiv:1212.5226v1 [astro-ph.CO].

Constraints from Planck[9]

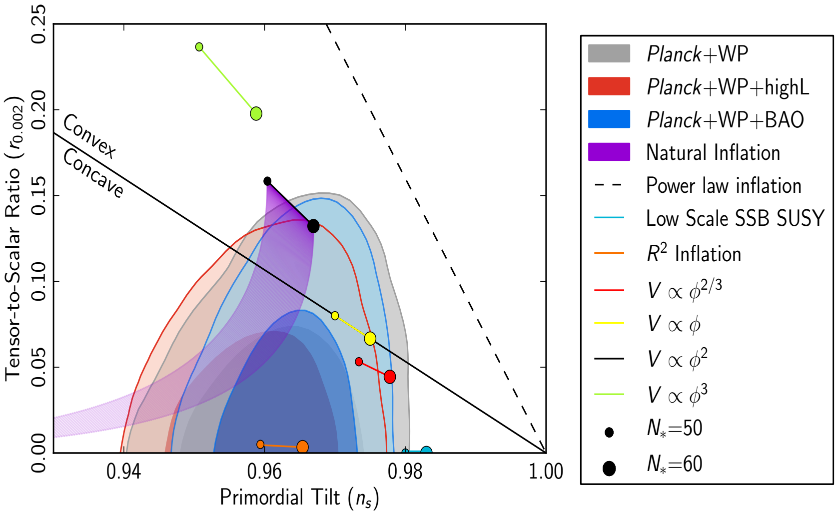

The corresponding constraints from the Planck data for various models.

[9] P. A. R. Ade *et al.*, arXiv:1303.5082 [astro-ph.CO].

Does the primordial power spectrum contain features?

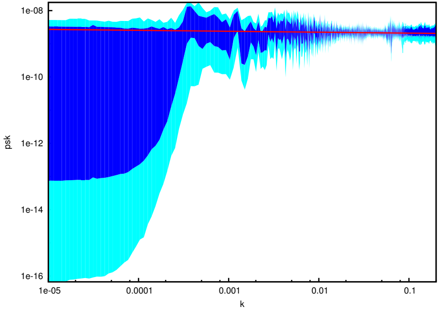

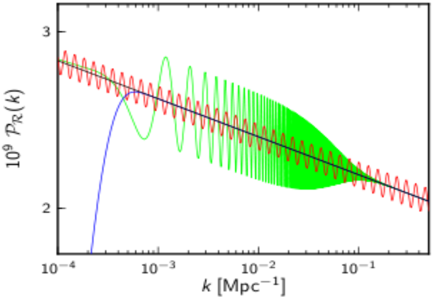

Left: Reconstructed primordial spectra, obtained upon assuming the concordant background ΛCDM model. Recovered spectra improve the fit to the WMAP nine-year data by $\Delta\chi^2_{\rm eff} \simeq 300$, with respect to the best fit power law spectrum[10].

Right: Three different spectra with features that lead to an improved fit (of $\Delta\chi^2_{\rm eff} \simeq 10$) to the Planck data[11].

[10] D. K. Hazra, A. Shafieloo and T. Souradeep, JCAP **1307**, 031 (2013).

[11] P. A. R. Ade *et al.*, arXiv:1303.5082 [astro-ph.CO].

Inflationary models permitting deviations from slow roll

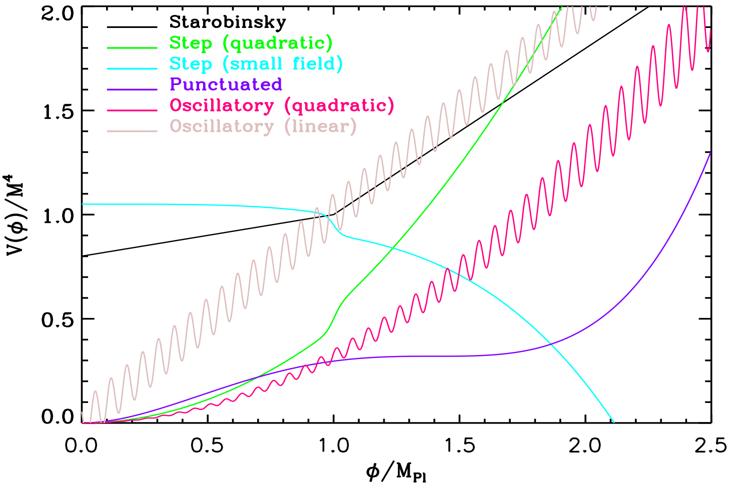

Illustration of potentials that admit departures from slow roll.

Spectra leading to an improved fit to the WMAP data

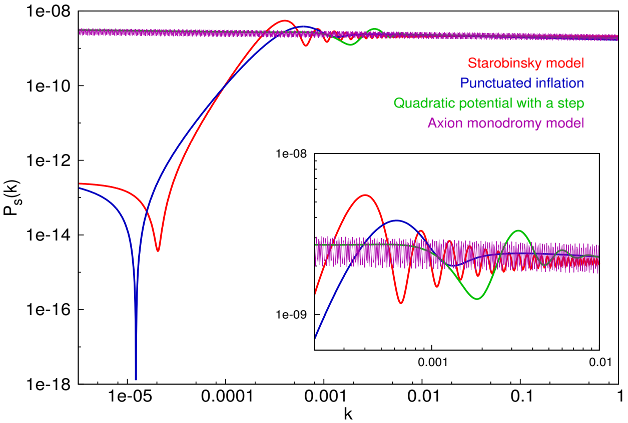

The scalar power spectra in the different inflationary models that lead to a better fit to the CMB data than the conventional power law spectrum[12].

[12] R. K. Jain, P. Chingangbam, J.-O. Gong, L. Sriramkumar and T. Souradeep, JCAP **0901**, 009 (2009); D. K. Hazra, M. Aich, R. K. Jain, L. Sriramkumar and T. Souradeep, JCAP **1010**, 008 (2010); M. Aich, D. K. Hazra, L. Sriramkumar and T. Souradeep, Phys. Rev. D **87**, 083526 (2013).

The scalar bi-spectrum

The scalar bi-spectrum $\mathcal{B}_{\mathcal{RRR}}(\boldsymbol{k}_1, \boldsymbol{k}_2, \boldsymbol{k}_3)$ is related to the three point correlation function of the Fourier modes of the curvature perturbation, evaluated towards the end of inflation, say, at the conformal time $\eta_{\rm e}$, as follows[13]:

$$\langle \hat{\mathcal{R}}_{\boldsymbol{k}_1}(\eta_{\rm e})\, \hat{\mathcal{R}}_{\boldsymbol{k}_2}(\eta_{\rm e})\, \hat{\mathcal{R}}_{\boldsymbol{k}_3}(\eta_{\rm e})\rangle = (2\,\pi)^3\; \mathcal{B}_{\mathcal{RRR}}(\boldsymbol{k}_1, \boldsymbol{k}_2, \boldsymbol{k}_3)\; \delta^{(3)}\left(\boldsymbol{k}_1 + \boldsymbol{k}_2 + \boldsymbol{k}_3\right).$$

For convenience, we shall set

$$\mathcal{B}_{\mathcal{RRR}}(\boldsymbol{k}_1, \boldsymbol{k}_2, \boldsymbol{k}_3) = (2\,\pi)^{-9/2}\; G_{\mathcal{RRR}}(\boldsymbol{k}_1, \boldsymbol{k}_2, \boldsymbol{k}_3).$$

[13] D. Larson *et al.*, Astrophys. J. Suppl. **192**, 16 (2011);
E. Komatsu *et al.*, Astrophys. J. Suppl. **192**, 18 (2011).

The non-Gaussianity parameter $f_{\rm NL}$

The observationally relevant non-Gaussianity parameter $f_{\rm NL}$ is basically introduced through the relation[14]

$$\mathcal{R}(\eta, \boldsymbol{x}) = \mathcal{R}_{\rm G}(\eta, \boldsymbol{x}) - \frac{3\, f_{\rm NL}}{5}\, \left[\mathcal{R}_{\rm G}^2(\eta, \boldsymbol{x}) - \left\langle \mathcal{R}_{\rm G}^2(\eta, \boldsymbol{x})\right\rangle\right],$$

where $\mathcal{R}_{\rm G}$ denotes the Gaussian quantity, and the factor of $3/5$ arises due to the relation between the Bardeen potential and the curvature perturbation during the matter dominated epoch.

Utilizing the above relation and Wick's theorem, one can arrive at the three-point correlation function of the curvature perturbation in Fourier space in terms of the parameter $f_{\rm NL}$. It is found to be

$$\begin{aligned}\langle \hat{\mathcal{R}}_{\boldsymbol{k}_1}\, \hat{\mathcal{R}}_{\boldsymbol{k}_2}\, \hat{\mathcal{R}}_{\boldsymbol{k}_3}\rangle \quad &= \quad -\frac{3\, f_{\rm NL}}{10}\, (2\,\pi)^{5/2}\, \left(\frac{1}{k_1^3\, k_2^3\, k_3^3}\right)\, \delta^{(3)}(\boldsymbol{k}_1 + \boldsymbol{k}_2 + \boldsymbol{k}_3) \\ &\quad \times \left[k_1^3\, \mathcal{P}_{\rm S}(k_2)\, \mathcal{P}_{\rm S}(k_3) + \text{two permutations}\right].\end{aligned}$$

[14] E. Komatsu and D. N. Spergel, Phys. Rev. D **63**, 063002 (2001).

The relation between $f_{_{\rm NL}}$ and the scalar bi-spectrum

Upon making use of the above expression for the three-point function of the curvature perturbation and the definition of the scalar bi-spectrum, we can, in turn, arrive at the following relation[15]:

$$\begin{aligned} f_{_{\rm NL}}(\boldsymbol{k}_1,\boldsymbol{k}_2,\boldsymbol{k}_3) &= -\frac{10}{3}\,(2\,\pi)^{1/2}\,\left(k_1^3\,k_2^3\,k_3^3\right)\,\mathcal{B}_{\mathcal{RRR}}(\boldsymbol{k}_1,\boldsymbol{k}_2,\boldsymbol{k}_3)\\ &\quad\times\,\left[k_1^3\,\mathcal{P}_{_{\rm S}}(k_2)\,\mathcal{P}_{_{\rm S}}(k_3)+\text{two permutations}\right]^{-1}\\ &= -\frac{10}{3}\,\frac{1}{(2\,\pi)^4}\,\left(k_1^3\,k_2^3\,k_3^3\right)\,G_{\mathcal{RRR}}(\boldsymbol{k}_1,\boldsymbol{k}_2,\boldsymbol{k}_3)\\ &\quad\times\,\left[k_1^3\,\mathcal{P}_{_{\rm S}}(k_2)\,\mathcal{P}_{_{\rm S}}(k_3)+\text{two permutations}\right]^{-1}. \end{aligned}$$

15 J. Martin and L. Sriramkumar, JCAP **1201**, 008 (2012).

The action at the cubic order

It can be shown that, the third order term in the action describing the curvature perturbation is given by[16]

$$\mathcal{S}^3_{\mathcal{R}\mathcal{R}\mathcal{R}}[\mathcal{R}] = \mathrm{M}^2_{_{\mathrm{Pl}}} \int \mathrm{d}\eta \int \mathrm{d}^3\boldsymbol{x} \biggl[a^2\,\epsilon_1^2\,\mathcal{R}\,\mathcal{R}'^2 + a^2\,\epsilon_1^2\,\mathcal{R}\,(\partial\mathcal{R})^2 - 2\,a\,\epsilon_1\,\mathcal{R}'\,(\partial^i\mathcal{R})\,(\partial_i\chi) + \frac{a^2}{2}\,\epsilon_1\,\epsilon_2'\,\mathcal{R}^2\,\mathcal{R}' + \frac{\epsilon_1}{2}\,(\partial^i\mathcal{R})\,(\partial_i\chi)\,(\partial^2\chi) + \frac{\epsilon_1}{4}\,(\partial^2\mathcal{R})\,(\partial\chi)^2 + \mathcal{F}_1\left(\frac{\delta\mathcal{L}^2_{\mathcal{R}\mathcal{R}}}{\delta\mathcal{R}}\right)\biggr],$$

where $\mathcal{F}_1(\delta\mathcal{L}^2_{\mathcal{R}\mathcal{R}}/\delta\mathcal{R})$ denotes terms involving the variation of the second order action with respect to $\mathcal{R}$, while χ is related to the curvature perturbation $\mathcal{R}$ through the relation

$$\partial^2\chi = a\,\epsilon_1\,\mathcal{R}'.$$

[16] J. Maldacena, JHEP **0305**, 013 (2003);
D. Seery and J. E. Lidsey, JCAP **0506**, 003 (2005);
X. Chen, M.-x. Huang, S. Kachru and G. Shiu, JCAP **0701**, 002 (2007).

Evaluating the scalar bi-spectrum

At the leading order in the perturbations, one then finds that the scalar three-point correlation function in Fourier space is described by the integral[17]

$$\langle\hat{\mathcal{R}}_{\boldsymbol{k}_1}(\eta_{\rm e})\,\hat{\mathcal{R}}_{\boldsymbol{k}_2}(\eta_{\rm e})\,\hat{\mathcal{R}}_{\boldsymbol{k}_3}(\eta_{\rm e})\rangle = -i\int_{\eta_{\rm i}}^{\eta_{\rm e}} {\rm d}\eta\; a(\eta)\;\left\langle\left[\hat{\mathcal{R}}_{\boldsymbol{k}_1}(\eta_{\rm e})\,\hat{\mathcal{R}}_{\boldsymbol{k}_2}(\eta_{\rm e})\,\hat{\mathcal{R}}_{\boldsymbol{k}_3}(\eta_{\rm e}), \hat{H}_{\rm I}(\eta)\right]\right\rangle,$$

where $\hat{H}_{\rm I}$ is the Hamiltonian corresponding to the above third order action, while $\eta_{\rm i}$ denotes a sufficiently early time when the initial conditions are imposed on the modes, and $\eta_{\rm e}$ denotes a very late time, say, close to when inflation ends.

Note that, while the square brackets imply the commutation of the operators, the angular brackets denote the fact that the correlations are evaluated in the initial vacuum state (*viz.* the Bunch-Davies vacuum in the situation of our interest).

[17] See, for example, D. Seery and J. E. Lidsey, JCAP **0506**, 003 (2005); X. Chen, Adv. Astron. **2010**, 638979 (2010).

The various times of interest

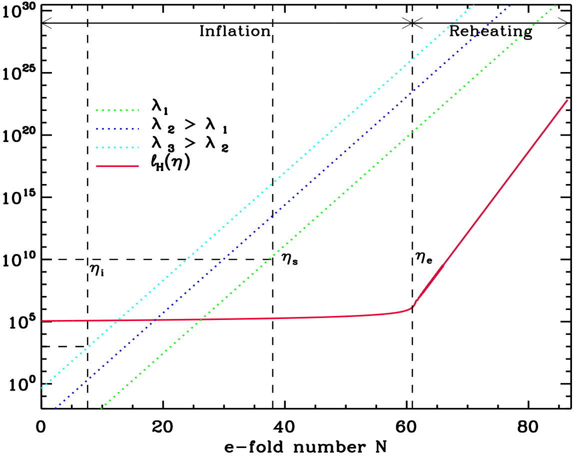

The exact behavior of the physical wavelengths and the Hubble radius plotted as a function of the number of e-folds in the case of the archetypical quadratic potential, which allows us to illustrate the various times of our interest, *viz.* $\eta_{\rm i}$, $\eta_{\rm s}$ and $\eta_{\rm e}$.

Results from BINGO

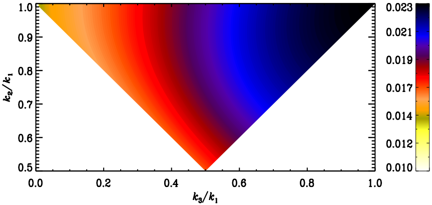

A comparison of the analytical results (on the left) for the non-Gaussianity parameter $f_{\rm NL}$ with the numerical results (on the right) from the BIspectra and Non-Gaussianity Operator (BINGO) code for a generic triangular configuration of the wavevectors in the case of the standard quadratic potential[18]. The maximum difference between the numerical and the analytic results is found to be about 5%.

[18] D. K. Hazra, L. Sriramkumar and J. Martin, JCAP **05**, 026 (2013).

Template bispectra

For comparison with the observations, the scalar bi-spectrum is often expressed as follows[19]:

$$G_{\mathcal{R}\mathcal{R}\mathcal{R}}(\boldsymbol{k}_1, \boldsymbol{k}_2, \boldsymbol{k}_3) = f_{\rm NL}^{\rm loc}\, G_{\mathcal{R}\mathcal{R}\mathcal{R}}^{\rm loc}(\boldsymbol{k}_1, \boldsymbol{k}_2, \boldsymbol{k}_3) + f_{\rm NL}^{\rm eq}\, G_{\mathcal{R}\mathcal{R}\mathcal{R}}^{\rm eq}(\boldsymbol{k}_1, \boldsymbol{k}_2, \boldsymbol{k}_3) + f_{\rm NL}^{\rm orth}\, G_{\mathcal{R}\mathcal{R}\mathcal{R}}^{\rm orth}(\boldsymbol{k}_1, \boldsymbol{k}_2, \boldsymbol{k}_3),$$

where $f_{\rm NL}^{\rm loc}$, $f_{\rm NL}^{\rm eq}$ and $f_{\rm NL}^{\rm orth}$ are free parameters that are to be estimated, and the local, the equilateral, and the orthogonal template bi-spectra are given by:

$$\begin{aligned}
G_{\mathcal{R}\mathcal{R}\mathcal{R}}^{\rm loc}(\boldsymbol{k}_1, \boldsymbol{k}_2, \boldsymbol{k}_3) &= \frac{6}{5}\left[\frac{(2\,\pi^2)^2}{k_1^3\,k_2^3\,k_3^3}\right]\left(k_1^3\,\mathcal{P}_{\rm S}(k_2)\,\mathcal{P}_{\rm S}(k_3) + \text{two permutations}\right),\\
G_{\mathcal{R}\mathcal{R}\mathcal{R}}^{\rm eq}(\boldsymbol{k}_1, \boldsymbol{k}_2, \boldsymbol{k}_3) &= \frac{3}{5}\left[\frac{(2\,\pi^2)^2}{k_1^3\,k_2^3\,k_3^3}\right)\left(6\,k_2\,k_3^2\,\mathcal{P}_{\rm S}(k_1)\,\mathcal{P}_{\rm S}^{2/3}(k_2)\,\mathcal{P}_{\rm S}^{1/3}(k_3) - 3\,k_3^3\,\mathcal{P}_{\rm S}(k_1)\,\mathcal{P}_{\rm S}(k_2)\right.\\
&\qquad \left. -2\,k_1\,k_2\,k_3\,\mathcal{P}_{\rm S}^{2/3}(k_1)\,\mathcal{P}_{\rm S}^{2/3}(k_2)\,\mathcal{P}_{\rm S}^{2/3}(k_3) + \text{five permutations}\right),\\
G_{\mathcal{R}\mathcal{R}\mathcal{R}}^{\rm orth}(\boldsymbol{k}_1, \boldsymbol{k}_2, \boldsymbol{k}_3) &= \frac{3}{5}\left[\frac{(2\,\pi^2)^2}{k_1^3\,k_2^3\,k_3^3}\right]\left(18\,k_2\,k_3^2\,\mathcal{P}_{\rm S}(k_1)\,\mathcal{P}_{\rm S}^{2/3}(k_2)\,\mathcal{P}_{\rm S}^{1/3}(k_3) - 9\,k_3^3\,\mathcal{P}_{\rm S}(k_1)\,\mathcal{P}_{\rm S}(k_2)\right.\\
&\qquad \left. -8\,k_1\,k_2\,k_3\,\mathcal{P}_{\rm S}^{2/3}(k_1)\,\mathcal{P}_{\rm S}^{2/3}(k_2)\,\mathcal{P}_{\rm S}^{2/3}(k_3) + \text{five permutations}\right).
\end{aligned}$$

The basis $(f_{\rm NL}^{\rm loc}, f_{\rm NL}^{\rm eq}, f_{\rm NL}^{\rm orth})$ for the scalar three-point function is considered to be large enough to encompass a range of interesting models.

[19] C. L. Bennett *et al.*, arXiv:1212.5225v1 [astro-ph.CO].

Illustration of the template bi-spectra

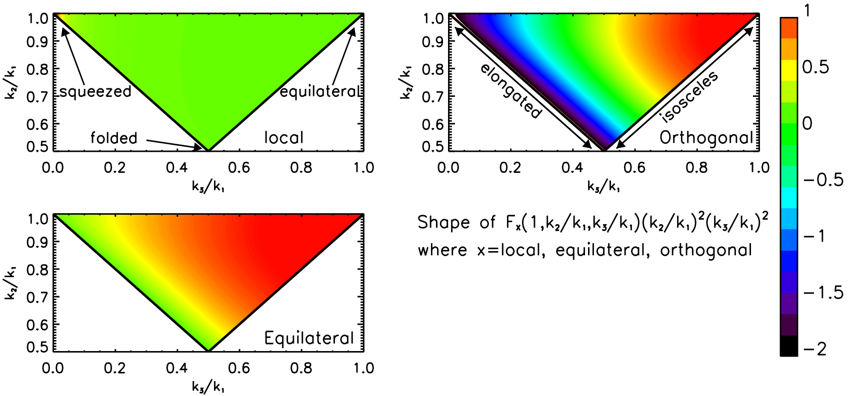

An illustration of the three template basis bi-spectra, *viz.* the local (top left), the equilateral (bottom) and the orthogonal (top right) forms for a generic triangular configuration of the wavevectors[20].

[20] E. Komatsu, Class. Quantum Grav. **27**, 124010 (2010).

Constraints on $f_{\rm NL}$

The constraints on the non-Gaussianity parameters from the recent Planck data are as follows[21]:

$$f_{\rm NL}^{\rm loc} = 2.7 \pm 5.8,$$
$$f_{\rm NL}^{\rm eq} = -42 \pm 75,$$
$$f_{\rm NL}^{\rm orth} = -25 \pm 39.$$

It should be stressed here that these are constraints on the primordial values.

Also, the constraints on each of the $f_{\rm NL}$ parameters have been arrived at assuming that the other two parameters are zero.

We should also add that these constraints become less stringent if the primordial spectra are assumed to contain features.

[21] P. A. R. Ade *et al.*, arXiv:1303.5084 [astro-ph.CO].

$f_{\rm NL}^{\rm loc}$ in models with a step

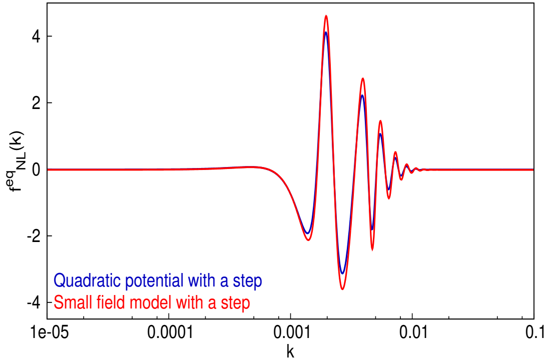

The non-Gaussianity parameter $f_{\rm NL}^{\rm loc}$ evaluated in the equilateral limit when a step has been introduced in the conventional chaotic inflationary model[22] involving the quadratic potential (in blue). The $f_{\rm NL}^{\rm loc}$ that arises in a small field model with a step[23] has also been illustrated (in red).

[22] X. Chen, R. Easther and E. A. Lim, JCAP **0706**, 023 (2007); JCAP **0804**, 010 (2008); P. Adshead, W. Hu, C. Dvorkin and H. V. Peiris, Phys. Rev. D **84**, 043519 (2011); P. Adshead, C. Dvorkin, W. Hu and E. A. Lim, Phys. Rev. D **85**, 023531 (2012).

[23] D. K. Hazra, L. Sriramkumar and J. Martin, JCAP **05**, 026 (2013).

$f_{\rm NL}^{\rm loc}$ in the axion monodromy model

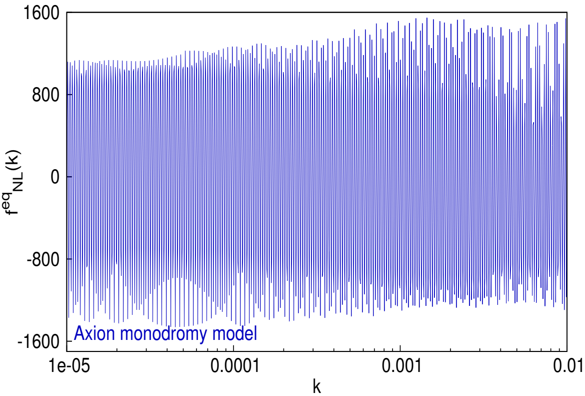

The non-Gaussianity parameter $f_{\rm NL}^{\rm loc}$ evaluated in the equilateral limit in the axion monodromy model[24].The modulations in the potential give rise to a certain resonant behavior[25], leading to a large $f_{\rm NL}^{\rm loc}$.

[24] D. K. Hazra, L. Sriramkumar and J. Martin, JCAP **05**, 026 (2013).

[25] S. Hannestad, T. Haugbolle, P. R. Jarnhus and M. S. Sloth, JCAP **1006**, 001 (2010); R. Flauger and E. Pajer, JCAP **1101**, 017 (2011).

The cross-correlations and the tensor bi-spectrum

The cross-correlations involving two scalars and a tensor and a scalar and two tensors are defined as

$$\langle \hat{\mathcal{R}}_{\boldsymbol{k}_1}(\eta_{\rm e})\, \hat{\mathcal{R}}_{\boldsymbol{k}_2}(\eta_{\rm e})\, \hat{\gamma}^{\boldsymbol{k}_3}_{m_3 n_3}(\eta_{\rm e})\,\rangle = (2\,\pi)^3\, \mathcal{B}^{m_3 n_3}_{\mathcal{R}\mathcal{R}\gamma}(\boldsymbol{k}_1,\boldsymbol{k}_2,\boldsymbol{k}_3)\; \delta^{(3)}\left(\boldsymbol{k}_1+\boldsymbol{k}_2+\boldsymbol{k}_3\right),$$

$$\langle \hat{\mathcal{R}}_{\boldsymbol{k}_1}(\eta_{\rm e})\, \hat{\gamma}^{\boldsymbol{k}_2}_{m_2 n_2}(\eta_{\rm e})\, \hat{\gamma}^{\boldsymbol{k}_3}_{m_3 n_3}(\eta_{\rm e})\rangle = (2\,\pi)^3\, \mathcal{B}^{m_2 n_2 m_3 n_3}_{\mathcal{R}\gamma\gamma}(\boldsymbol{k}_1,\boldsymbol{k}_2,\boldsymbol{k}_3) \times \delta^{(3)}\left(\boldsymbol{k}_1+\boldsymbol{k}_2+\boldsymbol{k}_3\right),$$

while the tensor bi-spectrum is given by

$$\langle \hat{\gamma}^{\boldsymbol{k}_1}_{m_1 n_1}(\eta_{\rm e})\, \hat{\gamma}^{\boldsymbol{k}_2}_{m_2 n_2}(\eta_{\rm e})\, \hat{\gamma}^{\boldsymbol{k}_3}_{m_3 n_3}(\eta_{\rm e})\rangle = (2\,\pi)^3\, \mathcal{B}^{m_1 n_1 m_2 n_2 m_3 n_3}_{\gamma\gamma\gamma}(\boldsymbol{k}_1,\boldsymbol{k}_2,\boldsymbol{k}_3) \times \delta^{(3)}\left(\boldsymbol{k}_1+\boldsymbol{k}_2+\boldsymbol{k}_3\right).$$

As in the pure scalar case, we shall set

$$\mathcal{B}_{\rm ABC}(\boldsymbol{k}_1,\boldsymbol{k}_2,\boldsymbol{k}_3) = (2\,\pi)^{-9/2}\; G_{\rm ABC}(\boldsymbol{k}_1,\boldsymbol{k}_2,\boldsymbol{k}_3),$$

where each of $({\rm A},{\rm B},{\rm C})$ can be either a $\mathcal{R}$ or a γ.

The corresponding non-Gaussianity parameters

As in the scalar case, one can define dimensionless non-Gaussianity parameters to characterize the scalar-scalar-tensor and the scalar-tensor-tensor cross-correlations and the tensor bi-spectrum, respectively, as follows:

$$C_{_{\rm NL}}^{\mathcal{R}} = -\frac{4}{(2\,\pi^2)^2}\,\left[k_1^3\,k_2^3\,k_3^3\,G_{\mathcal{R}\mathcal{R}\gamma}^{m_3 n_3}(\boldsymbol{k}_1,\boldsymbol{k}_2,\boldsymbol{k}_3)\right] \times \left(\Pi_{m_3 n_3,\bar{m}\bar{n}}^{\boldsymbol{k}_3}\right)^{-1}\,\left\{\left[k_1^3\,\mathcal{P}_{_{\rm S}}(k_2)+k_2^3\,\mathcal{P}_{_{\rm S}}(k_1)\right]\,\mathcal{P}_{_{\rm T}}(k_3)\right\}^{-1},$$

$$C_{_{\rm NL}}^{\gamma} = -\frac{4}{(2\,\pi^2)^2}\,\left[k_1^3\,k_2^3\,k_3^3\,G_{\mathcal{R}\gamma\gamma}^{m_2 n_2 m_3 n_3}(\boldsymbol{k}_1,\boldsymbol{k}_2,\boldsymbol{k}_3)\right] \times \left\{\mathcal{P}_{_{\rm S}}(k_1)\,\left[\Pi_{m_2 n_2,m_3 n_3}^{\boldsymbol{k}_2}\,k_3^3\,\mathcal{P}_{_{\rm T}}(k_2)+\Pi_{m_3 n_3,m_2 n_2}^{\boldsymbol{k}_3}\,k_2^3\,\mathcal{P}_{_{\rm T}}(k_3)\right]\right\}^{-1},$$

$$h_{_{\rm NL}} = -\left(\frac{4}{2\,\pi^2}\right)^2\,\left[k_1^3\,k_2^3\,k_3^3\,G_{\gamma\gamma\gamma}^{m_1 n_1 m_2 n_2 m_3 n_3}(\boldsymbol{k}_1,\boldsymbol{k}_2,\boldsymbol{k}_3)\right] \times \left[\Pi_{m_1 n_1,m_2 n_2}^{\boldsymbol{k}_1}\,\Pi_{m_3 n_3,\bar{m}\bar{n}}^{\boldsymbol{k}_2}\,k_3^3\,\mathcal{P}_{_{\rm T}}(k_1)\,\mathcal{P}_{_{\rm T}}(k_2)+\text{five permutations}\right]^{-1},$$

where the quantity $\Pi_{m_1 n_1,m_2 n_2}^{\boldsymbol{k}}$ is defined as

$$\Pi_{m_1 n_1,m_2 n_2}^{\boldsymbol{k}} = \sum_s\,\varepsilon_{m_1 n_1}^{s}(\boldsymbol{k})\,\varepsilon_{m_2 n_2}^{s*}(\boldsymbol{k}).$$

The actions governing the three point functions

The actions that lead to the correlations involving two scalars and one tensor, one scalar and two tensors and three tensors are given by

$$S^3_{\mathcal{R}\mathcal{R}\gamma}[\mathcal{R},\gamma_{ij}] = \mathrm{M}_{_{\mathrm{Pl}}}^2 \int \mathrm{d}\eta \int \mathrm{d}^3\boldsymbol{x}\, \biggl[a^2\,\epsilon_1\,\gamma_{ij}\,\partial_i\mathcal{R}\,\partial_j\mathcal{R} + \frac{1}{4}\,\partial^2\gamma_{ij}\,\partial_i\chi\,\partial_j\chi + \frac{a\,\epsilon_1}{2}\,\gamma_{ij}'\,\partial_i\mathcal{R}\,\partial_j\chi + \mathcal{F}^2_{ij}(\mathcal{R})\,\frac{\delta\mathcal{L}^2_{\gamma\gamma}}{\delta\gamma_{ij}} + \mathcal{F}^3(\mathcal{R},\gamma_{ij})\,\frac{\delta\mathcal{L}^2_{\mathcal{R}\mathcal{R}}}{\delta\mathcal{R}}\biggr],$$

$$S^3_{\mathcal{R}\gamma\gamma}[\mathcal{R},\gamma_{ij}] = \frac{\mathrm{M}_{_{\mathrm{Pl}}}^2}{4} \int \mathrm{d}\eta \int \mathrm{d}^3\boldsymbol{x}\, \biggl[\frac{a^2\,\epsilon_1}{2}\,\mathcal{R}\,\gamma_{ij}'\,\gamma_{ij}' + \frac{a^2\,\epsilon_1}{2}\,\mathcal{R}\,\partial_l\gamma_{ij}\,\partial_l\gamma_{ij} - a\,\gamma_{ij}'\,\partial_l\gamma_{ij}\,\partial_l\chi + \mathcal{F}^4_{ij}(\mathcal{R},\gamma_{mn})\,\frac{\delta\mathcal{L}^2_{\gamma\gamma}}{\delta\gamma_{ij}}\biggr],$$

$$S^3_{\gamma\gamma\gamma}[\gamma_{ij}] = \frac{\mathrm{M}_{_{\mathrm{Pl}}}^2}{2} \int \mathrm{d}\eta \int \mathrm{d}^3\boldsymbol{x}\, \biggl[\frac{a^2}{2}\,\gamma_{lj}\,\gamma_{im}\,\partial_l\partial_m\gamma_{ij} - \frac{a^2}{4}\,\gamma_{ij}\,\gamma_{lm}\,\partial_l\partial_m\gamma_{ij}\biggr].$$

The quantities $\mathcal{L}^2_{\mathcal{R}\mathcal{R}}$ and $\mathcal{L}^2_{\gamma\gamma}$ are the second order Lagrangian densities comprising of two scalars and tensors which lead to the equations of motion.

Comparison for an arbitrary triangular configuration

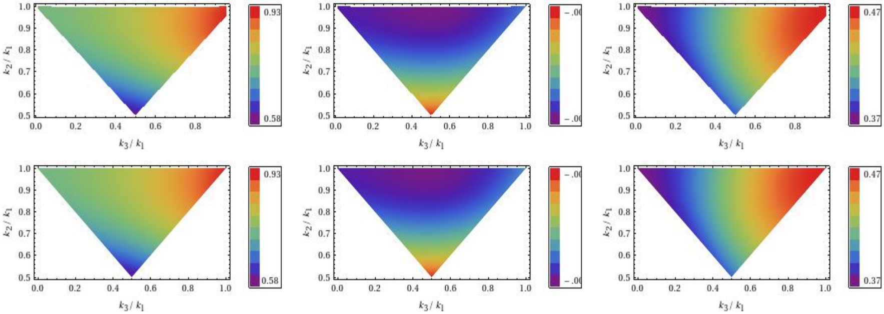

A comparison of the analytical results (at the bottom) for the non-Gaussianity parameters $C_{\rm NL}^{\mathcal{R}}$ (on the left), $C_{\rm NL}^{\gamma}$ (in the middle) and $h_{\rm NL}$ (on the right) with the numerical results (on top) for a generic triangular configuration of the wavevectors in the case of the standard quadratic potential[26]. As in the case of the scalar bi-spectrum, the maximum difference between the numerical and the analytic results is about 5%.

[26] V. Sreenath, R. Tibrewala and L. Sriramkumar, In preparation.

Three point functions for models with features

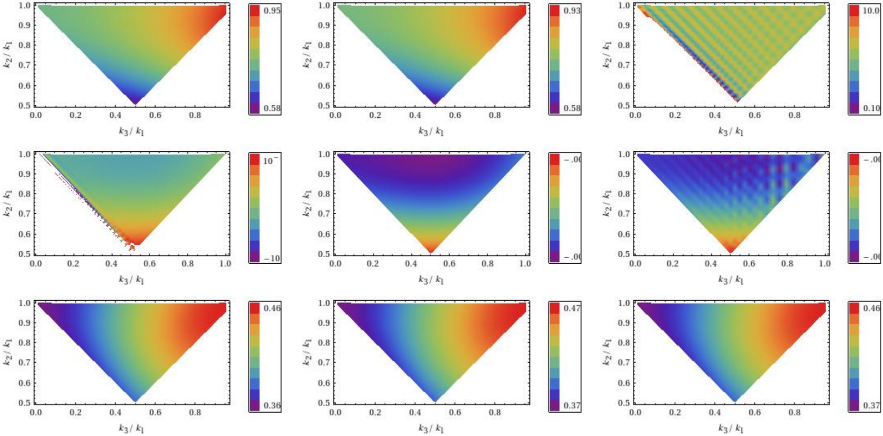

Density plots of the non-Gaussianity parameters $C_{\rm NL}^{\mathcal{R}}$ (on top), $C_{\rm NL}^{\gamma}$ (in the middle) and $h_{\rm NL}$ (at the bottom) evaluated numerically for an arbitrary triangular configuration of the wavenumbers for the case of the punctuated inflationary scenario (on the left), the quadratic potential with the step (in the middle) and the axion monodromy model (on the right).

Outlook

- The strong constraints on the non-Gaussianity parameter $f_{\rm NL}$ from Planck suggests that inflationary and post-inflationary scenarios that lead to rather large non-Gaussianities are very likely to be ruled out by the data.

[27] P. A. R. Ade *et al.*, arXiv:1303.5082 [astro-ph.CO].

[28] In this context, see, J. Martin, C. Ringeval and V. Vennin, arXiv:1303.3787 [astro-ph.CO].

[29] V. Sreenath, R. Tibrewala and L. Sriramkumar, In preparation.

Outlook

- The strong constraints on the non-Gaussianity parameter $f_{\rm NL}$ from Planck suggests that inflationary and post-inflationary scenarios that lead to rather large non-Gaussianities are very likely to be ruled out by the data.
- In contrast, various analyses seem to point to the fact that the scalar power spectrum may contain features[27].

[27] P. A. R. Ade *et al.*, arXiv:1303.5082 [astro-ph.CO].

[28] In this context, see, J. Martin, C. Ringeval and V. Vennin, arXiv:1303.3787 [astro-ph.CO].

[29] V. Sreenath, R. Tibrewala and L. Sriramkumar, In preparation.

Outlook

- The strong constraints on the non-Gaussianity parameter f_{NL} from Planck suggests that inflationary and post-inflationary scenarios that lead to rather large non-Gaussianities are very likely to be ruled out by the data.
- In contrast, various analyses seem to point to the fact that the scalar power spectrum may contain features[27].
- The possibility of such features can provide a strong handle on constraining inflationary models.

[27] P. A. R. Ade *et al.*, arXiv:1303.5082 [astro-ph.CO].

[28] In this context, see, J. Martin, C. Ringeval and V. Vennin, arXiv:1303.3787 [astro-ph.CO].

[29] V. Sreenath, R. Tibrewala and L. Sriramkumar, In preparation.

Outlook

- The strong constraints on the non-Gaussianity parameter f_{NL} from Planck suggests that inflationary and post-inflationary scenarios that lead to rather large non-Gaussianities are very likely to be ruled out by the data.
- In contrast, various analyses seem to point to the fact that the scalar power spectrum may contain features[27].
- The possibility of such features can provide a strong handle on constraining inflationary models.
- Else, one may need to carry out a systematic search involving the scalar and the tensor power spectra[28], the scalar and the tensor bi-spectra and the cross correlations[29] to arrive at a small subset of viable inflationary models.

---

[27] P. A. R. Ade *et al.*, arXiv:1303.5082 [astro-ph.CO].

[28] In this context, see, J. Martin, C. Ringeval and V. Vennin, arXiv:1303.3787 [astro-ph.CO].

[29] V. Sreenath, R. Tibrewala and L. Sriramkumar, In preparation.

Thank you for your attention